

## Research Article

# Study on Sulfur and Water Resistance of Marine Ruthenium Catalyst

**Yan H, Li J\*, Fan X and Li S**

Beijing Key Laboratory of Regional Combined Air Pollution Control, Beijing University of Technology, Beijing, China

**\*Corresponding author:** Jian Li, Beijing Key Laboratory of Regional Combined Air Pollution Control, Beijing University of Technology, Beijing 100124, China**Received:** March 23, 2022; **Accepted:** April 01, 2022;**Published:** April 08, 2022**Abstract**

A series of ruthenium-based catalysts were prepared by impregnation method and co-precipitation method, and applied to the catalytic oxidation of NO in the fast SCR for NO<sub>x</sub> removal in marine diesel engines. The effects of different supports and preparation methods on their catalytic activity and anti-sulfur and water-resistant properties were investigated. The Brunauer-Emmett-Teller (BET), temperature programmed reduction (TPR) method, oxygen temperature programmed desorption (O<sub>2</sub>-TPD) method, and X-ray diffraction (XRD) were used to analyze and determine the specific surface area, redox performance and characterization of the samples and the dispersion of ruthenium on the surface. The modified Ru/Al-CeZr-2 catalyst had significantly improved its low temperature activity and sulfur resistance and water resistance. The activity remained around 40% with SO<sub>2</sub> and H<sub>2</sub>O existed for 120min. After sulfur and water cut off, the active energy recovered to 52%, which could meet the conditions of fast SCR. It provided an idea for the industrialization process of ship SCR technology.

**Keywords:** Component: NO catalytic oxidation; sulfur and water resistance; Ruthenium-based catalyst; Cerium zirconium solid solution

## Introduction

In the mode of transportation of goods in the world, sea transportation accounts for a large proportion and is the main mode of transportation in international trade, undertaking more than 95% of the world trade transportation volume [1,2]. Diesel engines are the main power plant of ships, and NO<sub>x</sub> is one of the main components of harmful emissions from marine diesel engines [3]. Nitrogen oxides can cause three global environmental problems, acid rain, greenhouse effect and ozone layer destruction [4]. Currently, the SCR system is one of the most popular and matures NO<sub>x</sub> treatment devices. However, the ship space is limited, which makes it difficult for traditional SCR technology to be applied in practice [5]. The study had found that at the front end of the denigration system, about 50% NO was oxidized into NO<sub>2</sub> by catalytic oxidation of flue gas, which was also known as fast SCR. The reaction rate was ten times that of standard SCR [6], which could increase the reaction space velocity and reduce the volume of catalyst reaction equipment, which was of great significance to solve the practical problem of difficult layout of SCR systems such as ships.

Currently NO oxidation catalyst mainly included molecular sieves, activated carbon, transition metal and precious metal oxide catalysts. Among them, transition metal oxidation catalysts had been widely studied due to their low price, but they were easily poisoned by SO<sub>2</sub> and H<sub>2</sub>O, while noble metal oxidation catalysts had good anti-poisoning effect, but their high price and lack of resources made them suffer in industrial applications. Yao Rui et al. [7] prepared a series of Mn-Co/TiO<sub>2</sub> catalysts by impregnation method, and investigated the effect of Ce doping on the catalytic oxidation activity of the catalyst. The oxidation efficiency could reach over 85% at 250°C, but after 300ppm SO<sub>2</sub> and 5% H<sub>2</sub>O were introduced, the catalyst was rapidly

inactivated within 3h. Peng Lili et al. [8] pointed out that cerium zirconium solid solution could improve the dispersion of active component Co on the catalyst surface and increase the specific surface area. The prepared CoO<sub>x</sub>-CeO<sub>x</sub>/ZrO<sub>2</sub> catalyst could achieve 80.9% oxidation rate of NO at 250°C. When 180ppm SO<sub>2</sub> was introduced, the catalyst activity could be stable for 1h, but it dropped rapidly after 60min, and it was basically completely deactivated after 3h, however, its anti-sulfur and anti-water performance had not been explored. Li et al. [9] studied the catalytic oxidation of NO by Ru catalysts under different carriers, and the results showed that the optimal load of Ru was 2%, and Ru/TiO<sub>2</sub> could maintain a certain NO oxidation activity after 40ppm SO<sub>2</sub> and 2.5% H<sub>2</sub>O were added.

This paper mainly focused on the research on catalysts that generated NO<sub>2</sub> in fast SCR systems. In the above studies, the roasting temperature of catalysts was mostly below 500°C, while marine diesel engines were divided into two-stroke diesel engines and four-stroke diesel engines. The exhaust temperature of four-stroke diesel engines could be higher than 400°C, and the maximum exhaust temperature of Marine diesel engines could not exceed 550°C [10]. SO<sub>2</sub> and H<sub>2</sub>O are important components of gases discharged from ships. Therefore, under the condition that sulfur dioxide and water existed at the same time, it was a major problem to ensure that the oxidation activity of the catalyst could still meet the conditions of fast SCR. Only by overcoming this difficulty could it be widely used in industry. So, in this paper, the activity, sulfur and water resistance of ruthenium based catalysts with different supports under high temperature roasting were studied and CeZr solid solution was selected as the support and further modified with Al. A series of Ru/Al-CeZr-X catalysts were prepared and tested in a fixed-bed microreactor, and the oxidation activity, sulfur resistance and water resistance of the catalysts were discussed.

## Materials and Methods

### Materials

Chemical reagents used in the experiment are:  $\text{SiO}_2$ ,  $\gamma\text{-Al}_2\text{O}_3$ ,  $\text{ZrO}_2$ ,  $\text{CeO}_2$ ,  $\text{TiO}_2$  (industrial products). The dispersed metal salts of  $\text{Ce}(\text{NO}_3)_3 \cdot 6\text{H}_2\text{O}$ ,  $\text{Zr}(\text{NO}_3)_4 \cdot 5\text{H}_2\text{O}$ ,  $\text{RuCl}_3 \cdot x\text{H}_2\text{O}$ ,  $\text{Cr}(\text{NO}_3)_3 \cdot 9\text{H}_2\text{O}$  serve as a source of support material that requires no further purification.

### Methods

**Preparation of carrier:** A certain amount of cerium nitrate and zirconium nitrate solid (molar ratio 2:1) was dissolved in deionized water, and stirred to transparent state in ultrasonic water bath at  $70^\circ\text{C}$ . 1mol/L sodium hydroxide solution was added to pH value of 12-13, stirred for 3h, and precipitated viscose was obtained. The solid solution carrier of cerium zirconium could be obtained after washing in the filtration device until  $\text{pH}=7$ , dried in oven at  $110^\circ\text{C}$  and roasted in muffle furnace at  $600^\circ\text{C}$  for 3h.

The prepared cerium-zirconium solid solution was mixed with  $\gamma\text{-Al}_2\text{O}_3$  (mass ratio 1:1), and physically grounded to obtain an Al-CeZr-0 carrier.

The Al-CeZr-1 composite carrier was prepared by co-precipitation method. A certain amount of solid cerium nitrate and zirconium nitrate (molar ratio 2:1) was dissolved in deionized water, and stirred to transparent state in ultrasonic water bath at  $70^\circ\text{C}$ .  $\gamma\text{-Al}_2\text{O}_3$  powder with mass ratio 1:1 of cerium zirconium solid solution was added. Slowly added 1mol/L sodium hydroxide solution to a pH value of 12-13, stirred for 3h, to get the precipitated viscous substance. Washed in the suction filter device until  $\text{pH}=7$ , dried in oven at  $110^\circ\text{C}$ , roasted in muffle oven at  $600^\circ\text{C}$  for 3h.

The Al-CeZr-2 composite carrier was prepared by co-precipitation method. A certain amount of cerium nitrate and zirconium nitrate solid (molar ratio 2:1) were dissolved in deionized water, stirred in an ultrasonic water bathed at  $70^\circ\text{C}$  to a transparent state, and slowly added 1mol/L sodium hydroxide solution to pH value of 12-13, added  $\gamma\text{-Al}_2\text{O}_3$  powder with a mass ratio of cerium zirconium solid solution (1:1), stirred for 3h, and obtained a precipitated viscous substance. Washed in a suction filtration device to  $\text{pH}=7$ , dried in an oven at  $110^\circ\text{C}$ , and roasted in a muffle furnace at  $600^\circ\text{C}$  for 3h.

**Preparation of ruthenium catalyst:** A certain amount of  $\text{RuO}_2$  solution (0.5%wt  $\text{RuO}_2$ ) was dissolved in deionized water, then  $\text{SiO}_2$ ,  $\gamma\text{-Al}_2\text{O}_3$ ,  $\text{ZrO}_2$ ,  $\text{CeO}_2$ ,  $\text{TiO}_2$  and the prepared composite carrier were added, stirred in ultrasonic water bath, and dried at  $110^\circ\text{C}$ . The required catalysts, namely  $\text{Ru}/\text{SiO}_2$ ,  $\text{Ru}/\gamma\text{-Al}_2\text{O}_3$ ,  $\text{Ru}/\text{ZrO}_2$ ,  $\text{Ru}/\text{CeO}_2$ ,  $\text{Ru}/\text{TiO}_2$ ,  $\text{Ru}/\text{CeZr}$ ,  $\text{Ru}/\text{Al-CeZr-0}$ ,  $\text{Ru}/\text{Al-CeZr-1}$ ,  $\text{Ru}/\text{Al-CeZr-2}$ , could be prepared by roasting at  $550^\circ\text{C}$  in muffle furnace. The burned catalyst was ground and crushed, screened to 20-40 mesh, and reserved.

### Catalytic activity measurement

The activity of NO catalyst was evaluated in a continuous flow fixed-bed catalytic reactor, which was composed of gas distribution, reaction and flue gas test. The air distribution part was composed of high pressure gas cylinder, mass flow controller and display, mixing tank. The simulated flue gas came from the high-pressure gas cylinder and entered the reactor after being mixed evenly by the

mixing tank. The reaction part was carried out in a quartz tube, the catalyst to be evaluated was fixed with high temperature resistant quartz wool, the top of the tube was plugged with a rubber stopper, a type thermocouple is placed vertically above the catalyst bed, and a temperature controller is used to control the temperature conditions required for the evaluation. The reaction test temperature range was  $160\text{-}420^\circ\text{C}$ . The simulated flue gas consists of inlet concentration  $\text{NO}$ : 700ppm,  $\text{O}_2$ : 5%,  $\text{N}_2$  as equilibrium gas,  $\text{SO}_2$ : 200ppm,  $\text{H}_2\text{O}$ : 5vol%. The reaction was carried out at atmospheric pressure with a space velocity (GHSV) of  $27000\text{h}^{-1}$ .

Measurement of NO catalytic oxidation activity. The  $\text{NO}_x$  concentration was detected by a 42i-HL ( $\text{NO-NO}_2\text{-NO}_x$ ) flue gas analyzer from Thermo Fisher Scientific, USA.

NO conversion rate was calculated by the concentration of NO before and after the reaction (assuming the same inlet and outlet gas volume):

$$\eta = \frac{C_0 - C_1}{C_0} \times 100\%$$

$\eta$ : NO conversion rate, %;

$C_0$ : NO concentration at reactor inlet, ppm;

$C_1$ : NO concentration at the outlet of the reactor, ppm.

### Catalyst characterization

The specific surface area and pore structure of the catalyst were tested on Gemini V specific surface area and porosity analyzer. The sample was degassed at  $110^\circ\text{C}$  for 1h before testing. BET and BJH methods were used to measure the specific surface area, pore volume and pore size of the samples.

$\text{H}_2$ -TPR was carried out on Auto Chem II 2920 chemisorption apparatus. The catalyst was pretreated at  $300^\circ\text{C}$  in  $\text{O}_2$  atmosphere for 1h, cooled by He gas to room temperature, and then infused with a mixture of 10%  $\text{H}_2$ -90% Ar. The temperature was heated to  $850^\circ\text{C}$  at a rate of  $10^\circ\text{C} \cdot \text{min}^{-1}$ , and the TCD detector was used for analysis.

$\text{O}_2$ -TPD is an important method to study the oxygen storage performance of catalysts. The experiment was conducted on Tp-5080 automatic multi-purpose adsorber. Weigh 100 mg of the sample into a quartz micro-reaction tube, raised it to  $300^\circ\text{C}$  in an air atmosphere and keep it for 30h. Then purged from He to room temperature, switched the atmosphere to  $\text{O}_2$  for 1h to achieve adsorption saturation, switched He purged for 30min, Desorption was then performed at a rate of  $10^\circ\text{C}/\text{min}$  to  $800^\circ\text{C}$ , and the TCD signal was detected.

The phase composition and crystal structure of the samples were characterized by XRD and D8 advance X-ray diffractometer. Cu Ka was used as the radiation source, the tube voltage was 35kV, the tube current was 35mA, and the scanning was carried out in the range of  $10\text{-}80^\circ$  at a speed of  $5^\circ/\text{min}$ .

## Experiment Results and Discussion

### Effect of support on catalytic oxidation of NO and resistance to sulfur and water by Ruthenium

The NO oxidation activity of the Ru-based catalyst was clearly dependent on the carrier. The comparison of the oxidation activity of the Ru-based catalysts of the different carriers was shown in Figure 2a, and the NO conversion rate first rose and then decreased with

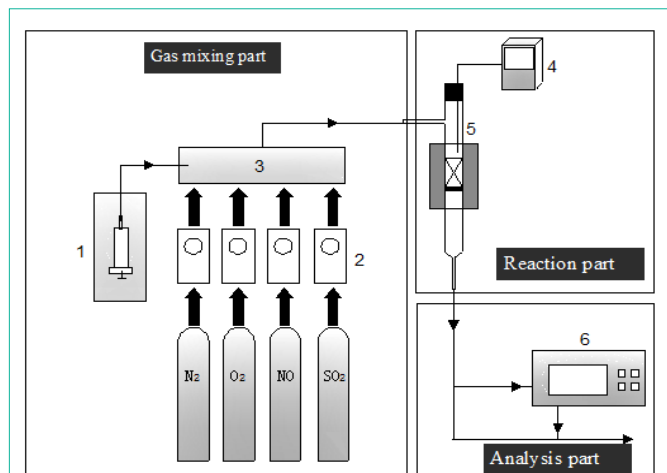


**Figure 1:** Flow diagram for laboratory experimental apparatus. (1) Syringe; (2) Gas flowmeter; (3) Mixing drum; (4) Temperature controller; (5) Quartz tube reactor; (6) Flue gas analyzer.

the increase of temperature, reached the maximum value at around 300°C. Among them, Ru/CeZr, Ru/CeO<sub>2</sub> and Ru/ZrO<sub>2</sub> obviously increased their oxidation efficiency at a low temperature of 220°C. It could be concluded from Figure 2a that the activity order of different carrier catalysts was loaded: Ru/CeZr> Ru/ZrO<sub>2</sub>> Ru/SiO<sub>2</sub>> Ru/ $\gamma$ -Al<sub>2</sub>O<sub>3</sub>> Ru/CeO<sub>2</sub>> Ru/TiO<sub>2</sub>. It could be seen that the Ru/CeZr catalyst had 79.51% of the highest oxidation activity at 280°C, which was lower than the best active temperature of the ruthenium catalyst with

different carriers, indicated that the Ru/CeZr catalyst had the optimal overall activity.

When SO<sub>2</sub> was present, its effect on the activity of a ruthenium-based catalyst with different oxide loads was investigated. The catalysts were stabilized for 60min under the temperature conditions when the catalysts had the best activity and then 200ppm SO<sub>2</sub> was introduced for 120min to conduct the experiment. It can be seen from Figure 2b that after SO<sub>2</sub> was introduced, the inactivation sequence within 120min was Ru/CeZr> Ru/ $\gamma$ -Al<sub>2</sub>O<sub>3</sub>> Ru/TiO<sub>2</sub>> Ru/SiO<sub>2</sub>> Ru/ZrO<sub>2</sub>> Ru/CeO<sub>2</sub>. The oxidation efficiency of Ru/ $\gamma$ -Al<sub>2</sub>O<sub>3</sub> and Ru/CeZr decreased relatively slowly after sulfuration. After 120min of sulfuration, Ru/ $\gamma$ -Al<sub>2</sub>O<sub>3</sub> was almost completely inactivated, and the activity of Ru/CeZr was 5%. The rest were completely inactivated within 30min of SO<sub>2</sub> penetration. The recovery of Ru/ $\gamma$ -Al<sub>2</sub>O<sub>3</sub> and Ru/CeZr was faster and higher than other recovery effects, but they did not recover to the original level. The toxic effect of SO<sub>2</sub> on Ru/ $\gamma$ -Al<sub>2</sub>O<sub>3</sub> was irreversible. This might be due to the competitive adsorption of SO<sub>2</sub>, NO and O<sub>2</sub> and the formation of sulfate species [11].

Figure 2c showed the apparent toxicity of 5vol% H<sub>2</sub>O to the catalysts. Stabilized for 60min at temperature conditions when each catalyst was best active, and then introduced 300min 5%vol of H<sub>2</sub>O for experiments. As can be seen from Figure 2c, the order of catalyst activity after H<sub>2</sub>O stabilization was Ru/ZrO<sub>2</sub>> Ru/SiO<sub>2</sub>> Ru/CeZr> Ru/ $\gamma$ -Al<sub>2</sub>O<sub>3</sub>> Ru/TiO<sub>2</sub>> Ru/CeO<sub>2</sub>. The catalyst activity quickly recovered to a high level after 10min of H<sub>2</sub>O stoppage, but did not return to the original activity, indicated that the toxic effect of H<sub>2</sub>O on the catalyst

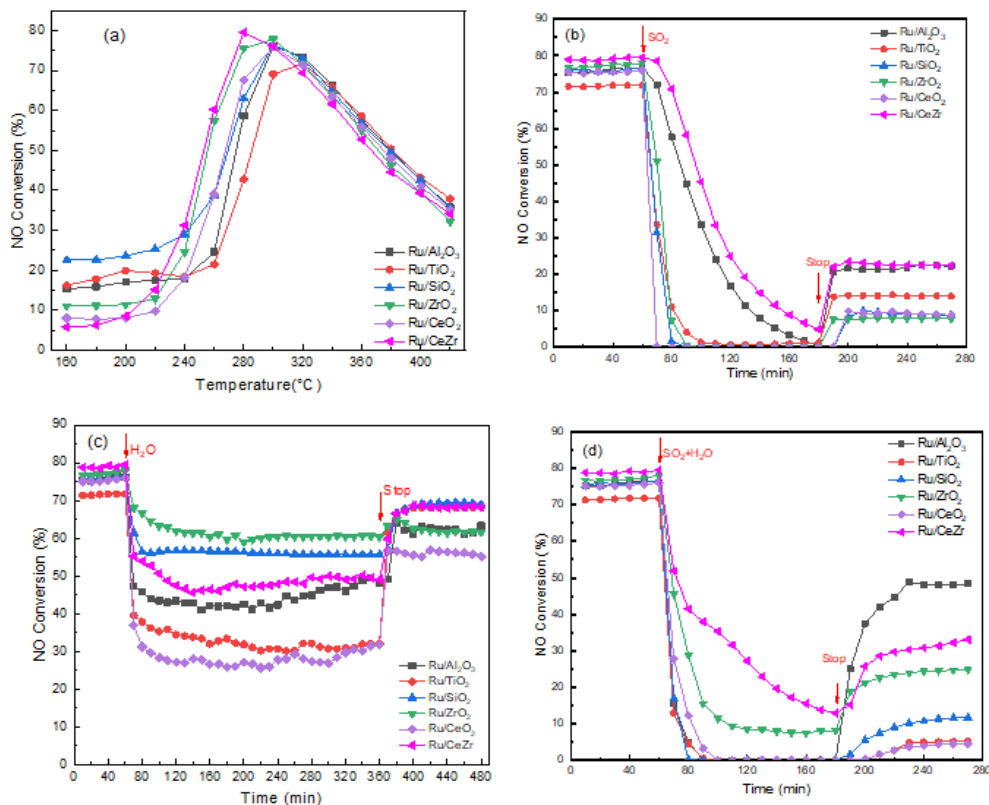


**Figure 2:** Effects of Supports on Ruthenium-Based Catalysts for NO Oxidation and resistance to sulfur and water. (a) Effect of the vector on the catalysts activity; (b) Effect of SO<sub>2</sub> on the catalysts activity; (c) Effect of H<sub>2</sub>O on the catalysts activity; (d) Effect of SO<sub>2</sub>+H<sub>2</sub>O on the catalysts activity.

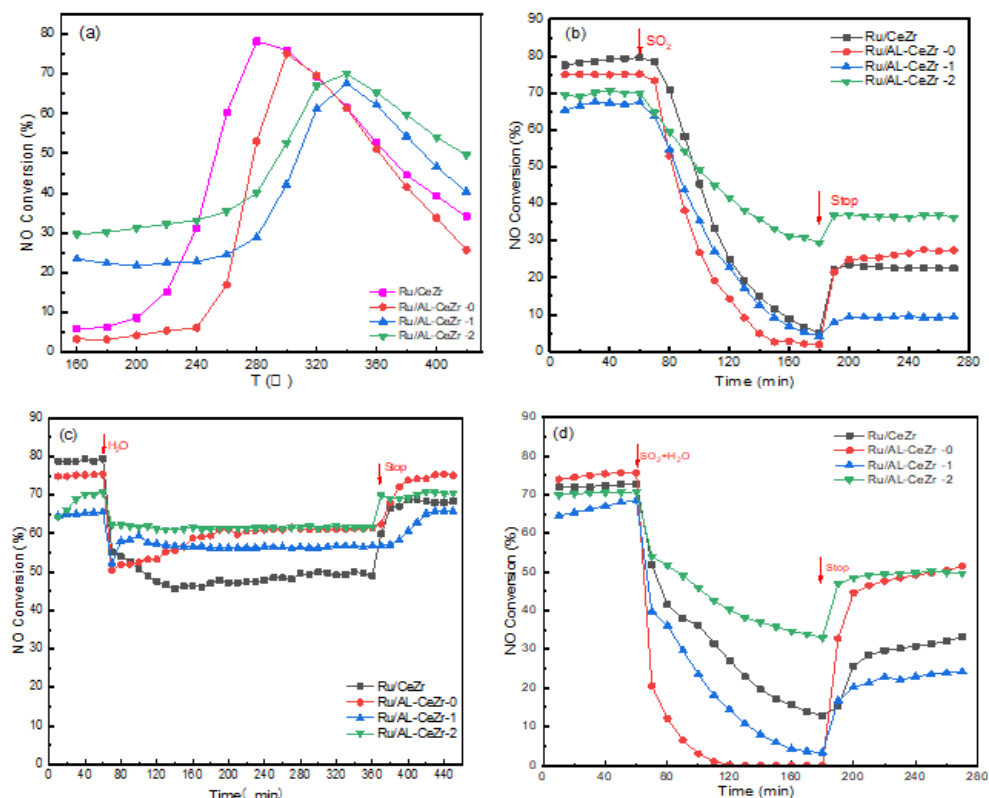


**Figure 3:** Effect of preparation method on ruthenium-based catalytic oxidation of NO and resistance to sulfur and water. (a) Effect of preparation method on the catalysts activity; (b) Effect of SO<sub>2</sub> on the catalysts activity; (c) Effect of H<sub>2</sub>O on the catalysts activity; (d) Effect of SO<sub>2</sub>+H<sub>2</sub>O on the catalysts activity.

was irreversible. One of the reasons for catalyst deactivation was the competitive adsorption of H<sub>2</sub>O with NO and O<sub>2</sub> [12]. Another reason might be that the strong oxidation capacity of the catalyst to NO led to the generation of a large number of NO<sub>2</sub>, which in turn generates nitrates with H<sub>2</sub>O, which couldn't be decomposed completely in time, and some undecomposed ones blocked the pores of the catalyst [13].

The effects of SO<sub>2</sub> and H<sub>2</sub>O on the activity of ruthenium catalysts supported by different oxides were investigated. Stabilized for 60min at temperature conditions when each catalyst was best active, and then 200ppm SO<sub>2</sub> and 5vol% H<sub>2</sub>O were added for 120min for experiment. It could be seen from Figure 2d that the catalyst activity of Ru/CeZr decreased to 42% after 20min, then slowly decreased, to 18% at 120min. For Ru/ZrO<sub>2</sub>, after 40min, the catalyst activity was decreased to 15%, followed by steady decline to 10%. The rest were almost completely inactivated after 40min of SO<sub>2</sub> and H<sub>2</sub>O penetration. As steam cut off, the activity of Ru/γ-Al<sub>2</sub>O<sub>3</sub> recovered to about 50%, which did not recover to the previous activity level, indicated that its toxic effect was irreversible. This might be because SO<sub>2</sub> will react with H<sub>2</sub>O and combine with the metal sites inside the catalyst to generate sulfate species, so that the metal oxide species that should be the active site was transformed into sulfate species, and sulfur poisoning phenomenon occurs on the catalyst to block the pores of the catalyst [14].

#### Effect of preparation method on catalytic oxidation of NO and sulfur and water resistance by Ruthenium

It could be seen from the catalytic activity and sulfur-water

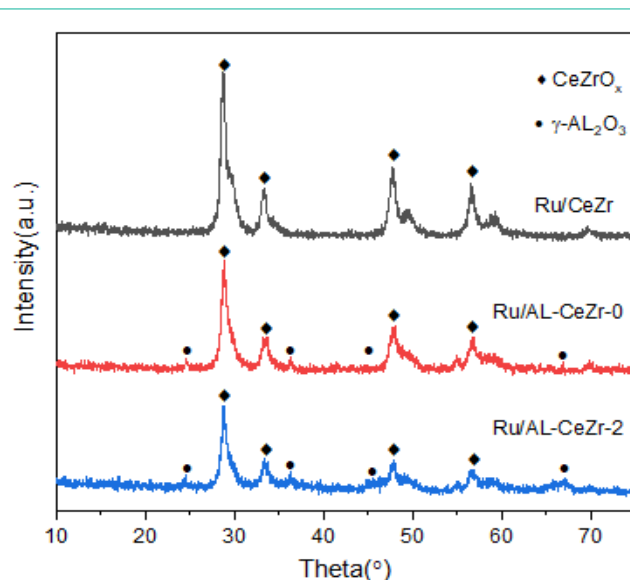


**Figure 4:** XRD patterns of Ru catalysts prepared by different methods.

resistance of ruthenium catalysts supported by different oxides that the ruthenium catalysts supported by CeZr solid solution and γ-Al<sub>2</sub>O<sub>3</sub> had better effects. Therefore, a composite support supported by 0.5%wt Ru catalyst with the mass ratio of γ-Al<sub>2</sub>O<sub>3</sub> and CeZr solid solution 1:1 was prepared. The following was called Ru/Al-CeZr-X, to explore its oxidation and sulfur and water resistance.

Figure 3a showed that the activity of ruthenium catalyst decreases after  $\gamma\text{-Al}_2\text{O}_3$  was added to the support. According to the Figure 3a, the best active order of the catalysts was Ru/CeZr > Ru/Al-CeZr-0 > Ru/Al-CeZr-2 > Ru/Al-CeZr-1. Although the maximum activity of Ru/Al-CeZr-1 and Ru/Al-CeZr-2 catalysts decreases, the activity of Ru/Al-CeZr-1 and Ru/Al-CeZr-2 catalysts increased significantly in the low temperature range of 160-240°C from 5% to about 23% and 29%. The activity of Ru/Al-CeZr-2 catalysts was also higher than the oxidation activity of Ru/CeZr after 340°C. The activity of Ru/Al-CeZr-2 catalyst was about 50% at 420°C, which could still meet the conditions of fast SCR reaction. It could be concluded that the modified Ru/Al-CeZr-X catalyst could improve the low temperature activity of the catalyst and reduce the activity decline rate in the high temperature region, so that it could still meet the conditions of fast SCR reaction in the high temperature region.

The effect of  $\text{SO}_2$  on the activity of Ru/Al-CeZr-X catalysts prepared by different methods was investigated. From Figure 3b we found that the activity of Ru/Al-CeZr-2 decreased the most slowly, and the catalytic activity of Ru/Al-CeZr-2 still maintained 30% after 120min, which was about 25% higher than that of Ru/CeZr. The recovery degree of Ru/Al-CeZr-2 was also the best, which could recover to about 38% after the sulfur removal. Compared with Ru/CeZr, the recovery ability of Ru/Al-CeZr-0 was improved to a certain extent, and the sulfur resistance and recovery ability of Ru/Al-CeZr-2 catalyst were improved greatly. The results indicated that the modified Ru/Al-CeZr-2 catalyst had better sulfur resistance.

The effect of  $\text{H}_2\text{O}$  on the activity of ruthenium catalysts supported by different oxides was investigated. As illustrated in Figure 3c, the sequence of activity after final stabilization was Ru/Al-CeZr-2 > Ru/Al-CeZr-0 > Ru/Al-CeZr-1 > Ru/CeZr. It showed that the water resistance of the catalysts after Al modification was improved, and the catalyst activity of Ru/Al-CeZr-2 tended to be stable at about 60% after passing  $\text{H}_2\text{O}$  for 10min. Compared with the activity before water, the activity was reduced by about 10%, and it had good water resistance. The activities of Ru/Al-CeZr-0 and Ru/Al-CeZr-1 catalysts both decreased first and then increased after passing through water. The former increased rapidly and finally stabilized at about 56%, while the latter increased slowly and stabilized at about 60%. After the water was stopped, all the catalysts modified by Al could recover to the previous activity level except Ru/CeZr, indicated that the toxic effect of  $\text{H}_2\text{O}$  on the activity of modified Ru/Al-CeZr-X catalyst was reversible.

The effects of  $\text{SO}_2$  and  $\text{H}_2\text{O}$  on the activity of ruthenium catalysts supported by different oxides were investigated. As could be seen from Figure 3d, compared with the toxic effect of  $\text{SO}_2$  alone, the catalyst was less toxic to the catalyst through  $\text{SO}_2$  and  $\text{H}_2\text{O}$  at the same time. This might be due to the competitive adsorption of  $\text{SO}_2$  and  $\text{H}_2\text{O}$ , which prevented massive adsorption of  $\text{SO}_2$  on the catalyst to form sulfate [15]. The main cause of catalyst deactivation was the formation of sulfate on the surface of the catalyst, blocked the pores of the catalyst. Due to the high sulfate decomposition temperature, the activity of the catalyst could not be restored to the original level after regeneration [16]. The activity of Ru/Al-CeZr-2 catalyst decreased the least, and the activity of Ru/Al-CeZr-2 catalyst remained about 40% after 120min, and the activity of Ru/Al-CeZr-2 catalyst recovered to 50% soon after  $\text{SO}_2$  and  $\text{H}_2\text{O}$  were stopped. The activity of Ru/Al-

CeZr-0 catalyst decreased the fastest, and was completely inactivated after 60min. However, after stopping the flow of  $\text{SO}_2$  and  $\text{H}_2\text{O}$ , its activity recovered the highest, which could recover to 52%, and had been in a recovery trend. Compared with Ru/CeZr and Ru/Al-CeZr-1, the activity of Ru/Al-CeZr-0 and Ru/Al-CeZr-2 catalysts could meet the conditions of fast SCR reaction after the cessation of  $\text{SO}_2$  and  $\text{H}_2\text{O}$ .

## Results of BET characterization

Table 1 compared the specific surface area and pore volume and pore diameter of ruthenium catalysts supported by different oxides. It could be seen that the results were not proportional to the oxidation activity of the catalysts. Therefore, the specific surface area and pore size of Ruthenium catalysts supported by different oxides had no decisive effect on their activity. Ru/ $\gamma\text{-Al}_2\text{O}_3$  catalyst had the largest specific surface area (196.02m<sup>2</sup>/g) and large pore volume (0.67cm<sup>3</sup>/g) pore size (13.74nm), but the oxidation activity of the catalyst was not the best. Ru/CeO<sub>2</sub>, Ru/ZrO<sub>2</sub> and Ru/CeZr catalysts with smaller specific surface area and pore volume data had the higher oxidation activity. This might be because the strong interaction between CeO<sub>2</sub> formed Ru-O-Ce, which reduced the activation energy of the reaction and promotes the reaction to proceed [17]. When ZrO<sub>2</sub> was used as catalyst carrier, composite oxide could be formed with the active component to improve the activity and stability of the catalyst [18]. Compared with pure zirconia and cerium oxide, cerium zirconium solid solution could significantly improve its thermal stability and oxygen storage performance, overcome the shortcomings of poor thermal stability at high temperature, and improve the service life and oxygen storage performance of the catalyst. Therefore, its catalytic activity was relatively good [19].

It could be seen from Table 2 that the BET surface area and pore volume and pore diameter of Ru/Al-CeZr-X catalyst were increased to a certain extent after Al modification, which might be directly influenced by the addition of  $\gamma\text{-Al}_2\text{O}_3$  in the carrier [20]. The BET surface area and pore volume and pore diameter of Ru/Al-CeZr-0 were small, and the data of Ru/Al-CeZr-1 and Ru/Al-CeZr-2 were obviously improved, which might be caused by the preparation method of Al-CeZr-X composite carrier. The coprecipitation method had larger BET surface area and pore size than the physical grinding method. However, the highest oxidation activity of Ru/Al-CeZr-X catalyst was lower than that of the modified Ru/CeZr catalyst, indicated that the oxidation performance of the catalyst was not directly related to the BET surface area and pore volume and pore diameter data.

## Results of XRD characterization

XRD patterns of Ru based catalysts prepared by different methods were shown in Figure 4. In the XRD patterns of Ru/CeZr, Ru/Al-CeZr-0 and Ru/Al-CeZr-2, the positions of solid solution exit peak of cerium zirconium solid solution were found to be 28.55°, 33.07°, 47.48° and 56.34° [21] (JCPDS38-1439). The peak positions of  $\gamma\text{-Al}_2\text{O}_3$  were 19.58°, 31.93°, 37.603°, 45.78°, 60.45° and 66.76° [22] (JCPDS29-0063). Only the CeZr solid solution and  $\gamma\text{-Al}_2\text{O}_3$  diffraction peaks corresponding to the carrier were observed, and no special peaks related to ceria, zirconia and ruthenium species were observed. It showed that the cerium zirconium solid solution was formed after roasting at high temperature, and the ruthenium element was well integrated into the lattice formed by cerium zirconium solid solution

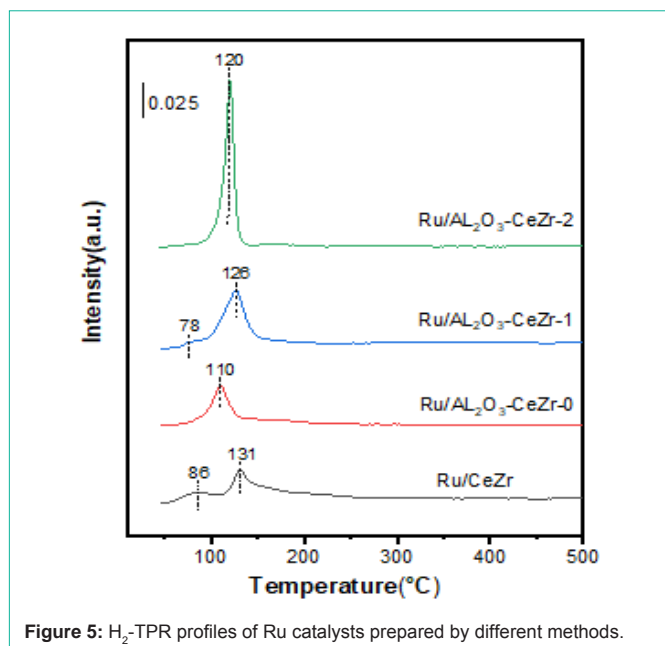


Figure 5: H<sub>2</sub>-TPR profiles of Ru catalysts prepared by different methods.

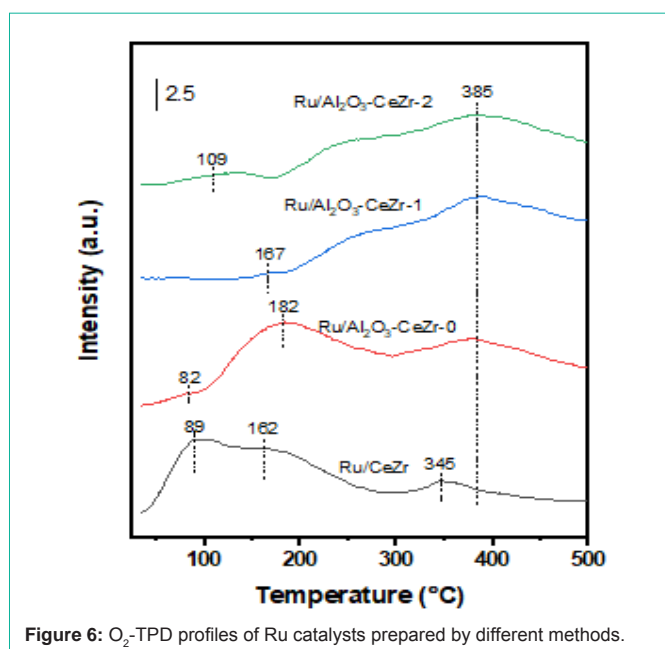


Figure 6: O<sub>2</sub>-TPD profiles of Ru catalysts prepared by different methods.

and  $\gamma$ -Al<sub>2</sub>O<sub>3</sub>, without changing the lattice structure of the carrier, and the dispersion degree on the carrier was very good.

### Results of H<sub>2</sub>-TPR characterization and O<sub>2</sub>-TPD characterization

Figure 5 showed the H<sub>2</sub>-TPR spectra of Ru-based catalysts prepared by different methods. As shown in Figure 5, the four samples all showed large reduction peaks at 90–180°C, and the reduction peaks within this range were mainly caused by the reduction of poorly crystallized or amorphous RuO<sub>x</sub> [23,24], which was consistent with the results of the XRD patterns. Compared with Ru/CeZr catalyst, it was obvious that the reduction peak of Al modified catalyst moved to the low temperature region, which could effectively improve its

Table 1: BET surface area and pore structure data of ruthenium catalysts with different supports.

Sample	Surface area/m <sup>2</sup> ·g <sup>-1</sup>	Pore volume/cm <sup>3</sup> ·g <sup>-1</sup>	Pore diameter/nm
Ru/Al <sub>2</sub> O <sub>3</sub>	196.02	0.67	13.74
Ru/TiO <sub>2</sub>	76.24	0.29	15.21
Ru/SiO <sub>2</sub>	145.1	0.75	20.58
Ru/ZrO <sub>2</sub>	3.24	0.01	12.6
Ru/CeO <sub>2</sub>	4.41	0.01	7.17
Ru/CeZr	54.7	0.12	8.87

Table 2: Different preparation methods Ru/Al-CeZr catalyst ratio surface area and pore structure data.

Sample	Surface area/m <sup>2</sup> ·g <sup>-1</sup>	Pore volume/cm <sup>3</sup> ·g <sup>-1</sup>	Pore diameter/nm
Ru/CeZr	54.7	0.12	8.87
Ru/Al-CeZr-0	76.64	0.28	11.31
Ru/Al-CeZr-1	127.18	2.5	58.69
Ru/Al-CeZr-2	126.66	0.53	14.22

redox capacity. It was worth noting that both Ru/CeZr and Ru/Al-CeZr-0 catalysts had small reduction peaks between 50–90°C, which were attributed to the reduction of atom-dispersed Ru<sup>+</sup>. Compared with crystallized RuO<sub>2</sub>, amorphous Ru species had better redox performance [25]. Ru/CeZr catalyst had a wide range of low temperature reduction peaks and a large peak area, so it had the higher oxidation activity.

In order to further evaluate the oxidation capacity of the catalyst, O<sub>2</sub>-TPD test was carried out. Because the oxygen adsorption process was carried out at room temperature, the peak at the lower temperature was attributed to the desorption of physical adsorption oxygen, while the peak at the higher temperature was attributed to the desorption of chemical adsorption oxygen. Since the redox capacity of catalysts was usually evaluated by surface chemisorbed oxygen resulting from the dissociation and adsorption of gaseous oxygen from oxygen vacancies on the catalyst surface. Compares the four curves in Figure 6, it could be seen that the first peak of the unmodified Ru/CeZr catalyst had the lowest starting temperature, and the peak area was significantly larger than that of The Ru/Al-CeZr-X catalyst, indicated that the surface oxygen was more likely to participate in the reaction and there were more oxygen species involved in the reaction, so the overall oxidation efficiency of the catalyst was higher. The starting temperature of the second peak was higher than that of Ru/Al-CeZr-X catalyst, and the peak area was also significantly smaller than that of Ru/Al-CeZr-X catalyst. It showed that the Ru/Al-CeZr-X catalyst can start the reaction at a lower temperature, corresponded to the improvement of its low temperature activity. This result was consistent with the oxidation efficiency results of the catalyst in Figure 3a.

### Conclusion

- The oxidation efficiency of Ru/CeZr catalyst prepared by roasting at 550°C reached 79% at 280°C. Compared with other oxide-supported ruthenium-based catalysts, the oxidation efficiency of Ru/CeZr was the highest after introducing SO<sub>2</sub> and H<sub>2</sub>O for 120min, which can reach 30%, and could recover to 35% after stopping SO<sub>2</sub> and H<sub>2</sub>O.

- The Ru/Al-CeZr-x series catalysts modified by adding Al to the Ru/CeZr catalyst could all recover to the previous activity level after stopping the H<sub>2</sub>O. The Ru/Al-CeZr-2 catalyst also greatly improved the low-temperature activity. The activity at 160°C was increased from 6% before modification to 30%. At the same time, the sulfur resistance and water resistance and the recovery performance after stopping sulfur and water were enhanced. The efficiency of Ru/Al-CeZr-2 catalyst could be maintained at 60% after supplying water for 300min, and the efficiency of introducing SO<sub>2</sub> and H<sub>2</sub>O for 120min was about 40%. After cutting off SO<sub>2</sub> and H<sub>2</sub>O, the oxidation activity could be restored to 52%, which could meet the reaction conditions of fast SCR. Fast SCR could improve the efficiency of standard SCR and reduced the volume of the catalyst, and provided an effective solution to the problem of insufficient space for ship SCR.

- It could be seen from the characterization results that Al modification could increase the specific surface area and pore size of the catalyst, and did not destroy the crystal lattice structure of the cerium zirconium solid solution, and improved the low temperature oxidation activity of the catalyst.

## Acknowledgments

This work was financially supported by the Demonstration of Multi-pollutant Medium and Low Temperature Collaborative Catalytic Purification Technology of National Key R&D Program (2I005013201801).

## References

- Nicholas NK. 50 Years of Review of Maritime Transport, 1968-2018: Reflecting on the Past, Exploring the Future. Geneva: United Nations Conference on Trade and Development. 2018.
- Huang WY, Huang WC, Zhu CC, et al. Numerical investigation on effect of catalyst on efficiency of SCR denitration of marine diesel engine. *Ship Engineering*. 2020; 42: 109-114.
- Wu Z, Chen YY, Cao L. Analysis of SCR key technology about marine diesel engine. *Diesel Engine*. 2015; 37: 20-23.
- Hao JM, Ma GD. *Air Pollution Control Engineering* [M]. BEIJING: Higher Education Press. 2010: 13-14.
- Xu W, Jiang DW, Ding L, et al. Shallow description ship SCR technology and its application. *Pearl River Water Transport*. 2009: 89-91.
- Kato A, Matsuda S, Kamo T, et al. Reaction between nitrogen oxide (NO<sub>x</sub>) and ammonia on iron oxide-titanium oxide catalyst. *The Journal of Physical Chemistry B*. 1981: 4099-4012.
- Yao R, Yin T, Bai ZL, et al. The effect of Ce-doping on NO catalytic oxidation on Mn-Co/TiO<sub>2</sub>. *Chemical World*. 2015; 56: 601-604+636.
- Peng LL, Huang Y, Li JG, et al. Catalytic performance of CoO<sub>x</sub>-CeO<sub>x</sub>/ZrO<sub>2</sub> in NO oxidation and its resistance against SO<sub>2</sub>. *Journal of Fuel Chemistry and Technology*. 2012; 40: 1377-1383.
- Li L, Qu L, Jie C, et al. Oxidation of nitric oxide to nitrogen dioxide over Ru catalysts. *Applied Catalysis B Environmental*. 2009; 88: 224-231.
- Luo WX. Application of SCR technology in diesel engine exhaust after treatment. *Science and Technology Innovation Herald*. 2020; 17: 63-65.
- Si M, Shen BX. The effect of SO<sub>2</sub> and O<sub>3</sub> on NO catalytic oxidation by manganese-cobalt catalyst. *Journal of HE BEI University of Technology*. 2021; 50: 69-76.
- Luo J, Tong H, Tong ZQ, et al. Low-Temperature catalytic reduction of NO over Cr-Ce/TiO<sub>2</sub> catalyst. *Petrochemical Technology*. 2010; 39: 1046-1051.
- Kulkarni AP, Muggli DS. The effect of water on the acidity of TiO<sub>2</sub> and sulfated titania. *Applied catalysis A General*. 2006; 302: 274-282.
- Du QW. Study on the CO-SCR performance of Mn-based catalysts and their resistance to H<sub>2</sub>O/SO<sub>2</sub>. *Shan Dong University*. 2021: 23-25.
- Peng LL, Huang Y, Li JG, et al. Catalytic performance of CoO<sub>x</sub>-CeO<sub>x</sub>/ZrO<sub>2</sub> in NO oxidation and its resistance against SO<sub>2</sub>. *Journal of Fuel Chemistry and Technology-China*. 2012; 40: 1377-1383.
- Sun Y, Huang Y, Zhao W, et al. Research on catalytic performance of supported perovskite catalyst for NO oxidation and resistance to SO<sub>2</sub> poisoning. *Journal of Fuel Chemistry and Technology*. 2014; 42: 1246-1252.
- Dai Q, Bai S, Wang Z, et al. Catalytic combustion of chlorobenzene over Ru-doped ceria catalysts. *Applied Catalysis B: Environmental*. 2012; 126: 64-75.
- Yang SM, Deng SH, Huang HM, et al. Application of zirconia supported catalyst. *Comments & Reviews in C.I.* 2003; 17: 1-4.
- Meng L. Research Progress on Synthesis of the CexZr1-xO<sub>2</sub> Oxygen Storage Materials. *Thermal Spray Technology*. 2021; 13: 85-94.
- Wang Y, Li ZQ, Fan RR, et al. Effect of cerium-zirconium solid solution on the performance of Pt-Pd/CexZryO<sub>2</sub>-Al<sub>2</sub>O<sub>3</sub> for diesel oxidation catalyst. *Metallic Functional Materials*. 2021; 28: 75-79+84.
- Mitsui T, Tsutsui K, Matsui T, et al. Catalytic abatement of acetaldehyde over oxide-supported precious metal catalysts. *Applied Catalysis B Environmental*. 2008; 78: 158-165.
- Lanza R, Jaras G, Canu P. Partial oxidation of methane over supported ruthenium catalysts. *Applied Catalysis a General*. 2007; 325: 57-67.
- Giles R, Cant NW, Kogel M, et al. The effect of SO<sub>2</sub> on the oxidation of NO over Fe-MFI and Fe-ferrierite catalysts made by solid-state ion exchange. *Applied Catalysis B Environmental*. 2000; 25: L75-L81.
- Nie XT, Ge QJ, Ma XG, et al. Preparation of cerium zirconium solid solution and CO oxidation performance of supported Au catalyst. *Natural Gas Chemical Industry*. 2013; 38: 6-11.
- Kong LP, Miao J, Li MH, et al. Study on denitration performance of CuMnCeLa-O/y-Al<sub>2</sub>O<sub>3</sub> catalyst for combustion. *Journal of Molecular Catalysis (China)*. 2018; 32: 295-304.